Journal of Physics:
Complexity

PAPER • **OPEN ACCESS**

Influence of model selection on optimal control of traffic for emissions minimisation

To cite this article: Khatun E Zannat *et al* 2025 *J. Phys. Complex.* **6** 035007

Journal of Physics: Complexity

PAPER

Influence of model selection on optimal control of traffic for emissions minimisation

Khatun E Zannat[1,*], **Judith Y T Wang**[1,2] **and David P Watling**[1]

[1] Institute for Transport Studies (ITS), University of Leeds, Woodhouse Lane, Leeds LS2 9JT, West Yorkshire, United Kingdom
[2] School of Civil Engineering, University of Leeds, Woodhouse Lane, Leeds LS2 9LG, West Yorkshire, United Kingdom
[*] Author to whom any correspondence should be addressed.

E-mail: K.E.Zannat@leeds.ac.uk, J.Y.T.Wang@leeds.ac.uk and D.P.Watling@its.leeds.ac.uk

Keywords: optimal traffic control, emission minimisation, traffic model, car-following model, traffic control strategy, emission measurement

Supplementary material for this article is available online

OPEN ACCESS

RECEIVED
30 December 2024

REVISED
6 June 2025

ACCEPTED FOR PUBLICATION
31 July 2025

PUBLISHED
14 August 2025

Abstract

The coupling of microscopic traffic simulation models with emission models offers a powerful tool for assessing and optimising traffic control strategies to reduce fuel consumption and vehicle emissions. Although many studies use traffic simulation for emission analysis and designing traffic control measures, most focus on calibrating a selected traffic model to replicate observed traffic flow. This raises a critical question: are the resulting optimal emission control strategies adequately designed to account for the sensitivity of traffic models in capturing vehicle dynamics and emissions? To address this issue, we compared three car-following models-the Krauss model, the Intelligent Driver Model, and the Wiedemann model-each rooted in distinct theoretical frameworks to understand traffic dynamics. We evaluated their performance in optimising road speed limits to minimise (PM_x) emissions in a school case study. A school was selected as the case because children are highly vulnerable and particularly exposed to pollutants during their school commute, and their exposure can be mitigated through optimal traffic control. Our findings reveal that, even when tuned to achieve comparable levels of traffic flow, the models displayed significant differences in their objective functions for traffic control optimisation. These discrepancies stemmed from variations in fuel consumption and particulate matter (PM_x) emission patterns resulting from the traffic dynamics captured by the selected traffic model. At a macroscopic level (e.g. average speed, flow, and density), the models exhibited minimal differences. However, at a microscopic level (e.g. acceleration, deceleration rates, and deviations from the mean), pronounced differences became evident. These results highlight that while certain traffic control strategies appeared less effective, revisiting and critically examining the limitations of the models is essential to ensure robust and tailored solutions for emission reduction.

1. Introduction

Road traffic, vital for the movement of passengers and goods, has been rapidly increasing in many parts of the world, leading to serious environmental and economic challenges (Din *et al* 2023). It is estimated that 70% of global CO_2 emissions are from urban areas, with transport and buildings being the largest contributors (United Nations 2024). Moreover, the traffic contribution to air pollution (particulate matter) varies from 5% to 61% in cities worldwide, with an average of 27% (Heydari *et al* 2020). The degradation of air quality caused by rising vehicular emissions in urban areas is now a major health concern. Emissions contribute to a range of health issues, including respiratory and cardiovascular diseases, and even premature deaths (Irin and Habib 2016). Populations in areas with a high number of active travellers and lower-income residents are especially exposed to elevated pollution levels (Li *et al* 2017, Xu *et al* 2019), with children and the elderly being particularly vulnerable (United Nations 2019).

The task of achieving an efficient traffic flow while lowering emissions has emerged as an important area of research, especially in crowded urban areas where congestion increases both environmental and economic burdens. To address these challenges, many cities are adopting traffic control strategies as part of sustainable transport planning—such as variable speed limits (Lee *et al* 2006, Khondaker and Kattan 2015), adaptive signal control (Midenet *et al* 2004, Day *et al* 2012), ramp metering (Grzybowska *et al* 2022), high-occupancy vehicle lanes (Cohen *et al* 2022) and congestion pricing (Zong *et al* 2024). However, the effectiveness of these control measures largely depends on the intricate interplay among the chosen control strategies, traffic conditions and their dynamics, and the robustness of the adopted modelling framework used to identify optimal solutions.

Advanced traffic management systems encompass traffic information, traffic assignment, traffic optimisation, and traffic prediction (Shahgholian and Gharavian 2018). Among these, traffic optimisation has been a critical link integrating the other components into a cohesive system aimed at improving flow, safety, and efficiency. When optimisation algorithms are applied for designing environmentally-focused traffic control measures, they strive to achieve the objective of reducing emissions indirectly through adapting the traffic flow. Optimisation algorithms in traffic control problems aim to determine the optimal values of decision variables, which represent the implementation of the optimal control policies to achieve the desired objectives. Evidence indicates that adopting optimal solutions such as optimum speeds tailored to road environments can lead to an 11% increase in travel time, 17% reduction in casualty crashes, and 7% to 18% decrease in air pollution emissions (Cameron 2022).

Despite the increasing interest in traffic control strategies aimed at reducing emissions, and in spite of numerous studies examining optimal control policies, the sensitivity analysis of optimal solutions based on selected sub-models—whether traffic models or emission models—remains a significantly understudied topic. Several critical gaps must be addressed to determine whether a given control measure is a worthwhile solution. This study aims to develop a more in-depth understanding of two key issues related to optimising traffic control measures for emissions reduction by:

(1) comparing the performance of different microscopic traffic models—specifically three car-following (CF) models of different genres—in measuring emissions.
(2) presenting a sensitivity analysis of optimal control solutions under various CF models used to simulate the vehicle trajectories.

The following section provides a detailed background justifying the need for this study and offers a critical evaluation of the selected approach. This is followed by a detailed description of the methodology and data analysis employed. The core section of the article presents a comprehensive report of the findings from the comparative analysis and sensitivity tests. Finally, the paper concludes with a discussion that integrates the key insights from the study and offers relevant policy recommendations for those tasked with designing optimal traffic control strategies to reduce emissions.

2. Literature review

This section aims to highlight relevant literature that supports the understanding of the study's primary research contributions.

2.1. Optimisation and traffic control strategies

Traffic control measures are a widely acknowledged tool for improving network performance through congestion reduction (Yan *et al* 2023, Göttlich *et al* 2024, Zhang *et al* 2024). In recent years, there has been an increasing focus on the development and application of optimisation-based traffic control strategies, driven by the dual objectives of improving traffic flow efficiency and minimising vehicle emissions. For instance, signal optimisation, whether for isolated intersections or coordinated networks, seeks to optimise parameters such as green time, red time, cycle length, phase sequences, and coordination to minimise delays, fuel consumption, and total emissions (Abudayyeh *et al* 2021, Jalili *et al* 2021). Similarly, speed limit optimisation aims to manage throughput and improve overall traffic and environmental outcomes (Zhang *et al* 2023). A somewhat different example is that of an optimised tolling strategy, which may be used to ensure the efficient utilisation of resources while also encouraging shifts in travel modes, driving routes, and departure times (Hasnine *et al* 2020). A diverse range of algorithms have been applied for determining optimal solutions, including heuristic and meta-heuristic methods (Shaikh *et al* 2020, Jalili *et al* 2021), exact approaches (Li *et al* 2011, Mohebifard and Hajbabaie 2019), and machine learning or artificial intelligence-based methods (Kővári *et al* 2022). While each optimisation approach has its limitations, the effectiveness and robustness of the solutions are highly dependent on the clarity of the problem definition and the accuracy of

the sub-models used to represent vehicular emissions, traffic characteristics, and their interactions. Hence, the success of optimisation efforts in determining policies that truly improve real-world conditions relies on the sensitivity and robustness of the underlying traffic and emission models. This highlights the critical need for a systematic evaluation of the factors influencing vehicular dynamics and emissions, in the context of environmentally-focused traffic control, in order to ensure the control measures actually deliver the anticipated improvements in the real-world.

2.2. Factors affecting vehicular emission

Vehicular emissions are influenced by a range of factors, including individual decisions, as well as vehicle-specific characteristics. For example, shifting from motorised transport to active modes such as cycling or walking can substantially reduce emissions, especially for short- to medium-distance trips (Rabl and De Nazelle 2012). Among various types of motorised vehicles—private cars, auto-rickshaws, and heavy- and light-duty vehicles—the emissions from private cars play a significant role in air pollution (Ajayi *et al* 2024). Global statistics indicate that private transport dominates transportation worldwide, with emissions from private cars contributing to 73% of urban air pollution (Lindau 2015). The type of engine and fuel also heavily impact emission levels. Diesel engines, for instance, emit higher levels of carbon monoxide (*CO*), hydrocarbons (*HC*), particulate matter (PM_x), and nitrogen oxides (NO_x) compared to gasoline engines (Kumar *et al* 2021). This is largely due to incomplete combustion and underutilised fuel, which release harmful chemicals into the atmosphere, disrupting ecosystems. In addition to vehicle conditions, driving behaviour, environmental factors, and weather conditions all affect emissions. Stop-and-go traffic, idling, aggressive driving (e.g. rapid acceleration and braking), and high speeds contribute to increased fuel consumption and emissions (Toledo 2007, Kousoulidou *et al* 2013, Rodríguez *et al* 2016, Gallus *et al* 2017, Llopis-Castelló *et al* 2018, Abdull *et al* 2020, Harrison *et al* 2021, Shang *et al* 2021). Therefore, to effectively reduce traffic-related emissions and implement control policies, it is crucial to investigate how vehicular maneuvering (e.g. speed, spacing, acceleration, deceleration) and different driving conditions (whether at an intersection, on highways, a congested downtown street, or in varying weather) contribute to pollution.

2.3. Traffic models in emission measurement

A key factor in accurate emission estimation lies in how effectively different traffic models capture vehicle dynamics, as this directly impacts the reliability of the optimum results. Modelling traffic flow allows a great variety of different traffic models - (1) macroscopic models are based on average quantities such as vehicle density and average flux (e.g. Lighthill Whitham and Richard model (Lighthill and Whitham 1955, Richards 1956), Payne-Whitham model (Payne 1971), Aw and Rascle's and Zhang' model (Aw and Rascle 2000, Zhang 2002)), (2) microscopic models describing individual vehicle dynamics (e.g. acceleration, lane changing and gap acceptance model (Toledo 2007)), and (3) meso-scopic models where individual vehicles moved according to dynamic laws that are governed by macroscopic rules (e.g. headway distribution models, cluster models, gas-kinetic models (Kessels and Kessels 2019)). Previous studies have used various traffic flow modelling frameworks to understand the traffic dynamics at different levels of resolution. While macroscopic traffic flow models have been often used for highway flow modelling (Kotsialos *et al* 2002, Ngoduy and Maher 2012), other studies have highlighted the suitability of microscopic traffic simulation for understanding urban local area traffic movement. One of the most important components of any microscopic traffic flow models is the CF model, which describes a vehicle's longitudinal behaviour and interactions with the leading vehicle or vehicles in the same lane. In essence, these models assume that drivers aim to control vehicle velocity to maintain a safe and comfortable following distance. The first CF model was developed around the 1950s by Reuschel (1950) and Pipes (1953), and since then a large number of CF models have been proposed. Depending on the focus of the development, they can be categorised as: stimulus-response model (e.g. Gazis-Herman-Rothery model (Gazis *et al* 1959), Optimal Velocity Model (Bando *et al* 1995), Intelligent Driver Model (IDM) (Treiber *et al* 2000), Tampere model (Tampère 2004)), a collision avoidance model (e.g. Pipes model (Pipes 1953), Gipps model (Gipps 1981), Krauss model (Krauss 1998)), a psycho-physical model (e.g. (Wiedemann 1974)), or an artificial intelligence model (e.g. fuzzy logic (McDonald *et al* 1997), neural network model (Panwai and Dia 2007), or combination of both). Each model is designed to handle a particular aspect of car-following behaviour, encompassing a separate set of assumptions, parameters, and intended usage. Research in the literature on emissions has attempted to predict traffic movement in urban areas by using traditional CF models (e.g. Song *et al* (2015) used Wiedemann'99 and Fritzsche models, Chauhan *et al* (2019) used Wiedemann 74 model), or by extending an already-existing model for that purpose (e.g. Meng *et al* (2021) used a modified Newell's model), or by developing a new, special purpose model (e.g. Meng *et al* (2024) proposed a new CF model considering the stochastic process of acceleration). While the availability of different models provides a wide range of investigation options for those wishing to control traffic flow, the wider choice also brings with it the

uncertainty as to the effect of model selection on the optimal policies. The empirical study by Song *et al* (2013) reveals that even after fine-tuning calibration, different CF models can produce varying emission estimates due to their differing abilities to accurately capture speed and acceleration dynamics. This finding underscores the importance of selecting an appropriate traffic model, as this choice may directly impact both the objective function and decision variables of an environmentally-focused optimisation problem.

2.4. Emission models and their sensitivity to traffic dynamics

Like the traffic model, the accuracy of emission estimates heavily depends on the capabilities of various emission models, as each model approaches the calculation of vehicular emissions in distinct ways. Efforts have been made to develop different emission models to measure emissions from traffic at various levels of resolution and complexity. Macroscopic emission models are based on parameters such as average driving speed and vehicle type, and are usually used to determine the impacts on a larger regional scale. COPERT (Abdull *et al* 2020, Ali *et al* 2021), MOBILE developed by US EPA (Koupal *et al* 2002), and EMission FACtor (EMFAC) developed by the California Air Resources Board (Bai *et al* 2009) are widely used macroscopic average speed models. Since these models are intended to predict emission inventories for large regional areas, they are not well suited for evaluating operational improvements that are more localised in nature, such as at signals, bottlenecks and on urban local roads (Scora and Barth 2006). Besides the average speed based approach, ARTEMIS (André 2004) and HBEFA (Colberg *et al* 2005, Notter *et al* 2021) both utilise the traffic situation (kinematics) while calculating emission factors. However, these models ignore the acceleration and deceleration of vehicles. On the other hand, microscopic emissions models such as VERSIT+ (Jie *et al* 2013), Comprehensive Modal Emissions Model (Scora and Barth 2006) and Passenger Car and Heavy Duty Emission Model (PHEM) (Wyatt *et al* 2014) estimate emissions based on second-by-second data on vehicle speed and acceleration patterns. Therefore, the effectiveness of the emissions' estimation and, by extension, of the optimisation model used to minimise emissions depend not only on the type of traffic model employed but also on the emission model's ability to capture variations in speed and acceleration and their potential impact on air pollution.

2.5. Microsimulation approach for emission control and traffic management strategies

Parallel to the advancements in traffic and emission models, recent years have witnessed a surge of interest in the transport field in utilising microsimulation tools to model traffic on road networks and to optimise traffic control measures. Microsimulation models are attractive for such analyses because they are based on the explicit representation of individual driver behaviours and the real-time space-time trajectories of individual vehicles. These models are able to capture the intricacies of vehicle trajectories, and provide vehicle operation data at high spatial and temporal resolution, including instantaneous speed and acceleration (Liu *et al* 2006, Madireddy *et al* 2011, Irin and Habib 2016). These vehicle operation data are essential inputs for detailed emission predcitions and thereby for optimisation models aimed at reducing emissions. Such models allow for the estimation of emissions both before and after the implementation of local traffic management interventions, such as signal timing optimisation or one-way traffic management. SUMO (Simulation of Urban MObility), VISSIM, AIMSUN are examples of such widely-used microsimulation tools used in such a context (Day *et al* 2012, De Coensel *et al* 2012, Alshayeb *et al* 2022). Research has shown that integrating microscopic traffic models, such as CF and lane-changing models, with emission models enables a more accurate quantification of the relationship between local traffic operations and emissions (Stevanovic *et al* 2009, Madireddy *et al* 2011, Irin and Habib 2016, Fan *et al* 2019, Zhao *et al* 2022).

2.6. Research gaps

While micro-simulation approaches are frequently employed to evaluate traffic control strategies by simulating traffic flow, it is a usual practice to select a single traffic model (Zhao *et al* 2019). Although comparative studies exist in the literature that compare predicted vehicular trajectories using different traffic models (Song *et al* 2013), there is limited consideration of how the choice of traffic model impacts emission measurements, or of the consequential impacts on traffic control measures aimed at reducing emissions. This gap raises a critical question: are current traffic control designs aimed at reducing emissions achieving genuinely optimal solutions, or are they constrained by the limitations of a particular traffic model?

As previously discussed, different CF models account for various aspects of driver behaviour, vehicle dynamics, and traffic characteristics. The assumptions in these models—such as how a vehicle accelerates, decelerates, or maintains a gap—directly impact on the prediction of emissions in the corresponding emission models, which could lead to significantly different outcomes in the design of emission control strategies. Through our experimental investigation in this study, we aimed to answer the following sequence of inter-linked research questions:

- To what extent do variations in the assumptions of a CF model lead to differences in emissions outputs?
- Are these emissions substantially different across different models?
- How does this variation impact optimal policy measures to minimise emissions?

In particular, we chose to investigate the minimisation of PM_x around a school area in the Bradford district, UK, achieved by applying speed control measures. A school was selected as the case because children are highly vulnerable and particularly exposed to pollutants during their school commute, and their exposure can be mitigated through optimal traffic control.

3. Methodology

This study aims to investigate the sensitivity of traffic control measures designed under various CF models. A specific focus was placed on evaluating the objective function of the optimisation model, and optimal solutions at a point of interest: Shipley C.E. Primary School in the Bradford District, United Kingdom. This location was chosen due to its strategic position along Otley Road, a major thoroughfare with high vehicular traffic intersecting Bradford Road (see figure 1). The methodology consists of five key stages: (1) Defining the optimisation problem, (2) Selecting models for traffic simulation, (3) Pairing the traffic simulation with a suitable emissions model, (4) Designing experiments to analyse emissions estimates, and (5) Comparing different traffic models to identify optimal strategies for emission reduction near the school. The ultimate aim was to gain insights into the robustness of traffic control strategies for urban emissions management with respect to the traffic model selection.

3.1. Optimisation problem

In our study, we focused on the problem of minimising emissions via optimising the speed limit. Hence, given a fine, discretised time-scale of the problem, the optimisation problem can be expressed as:

$$\min_{v_{limit}} \sum_{i=1}^{N} \sum_{t=1}^{T} E_i(t)\,\Delta t. \tag{1}$$

Here, $E_i(t)$ is the instantaneous emissions of PM_x for vehicle i during time step t. The decision variable (speed limit) must adhere to the practical and legal constraints for local roads i.e. $v_{min} \leqslant v_{limit} \leqslant v_{max}$. The total emissions of PM_x during the simulation period T depends on the sub-models (traffic model and emissions model) that translate the impact of the speed limit during the traffic flow simulation and emission estimation.

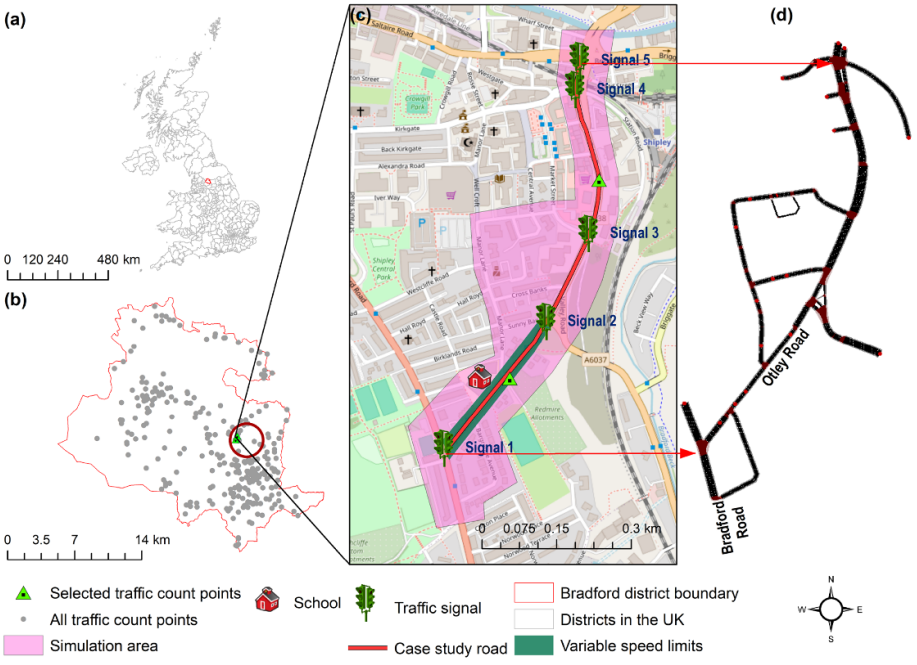

Figure 1. Study location and simulation area.

3.2. Selection of traffic model

The selection of a suitable model for local-level emission measurement is influenced by several factors to ensure it accurately represents traffic conditions and produces reliable emission estimates. In our study, a CF model was deemed appropriate, as emissions at the local scale of the case-study are particularly sensitive to stop-and-go traffic patterns, congestion, and queuing. For this research, we selected three well-established CF models, representative of different families of models: the Krauss model, from the collision avoidance family; the IDM, from the stimulus-response family; and the Wiedemann model, representative of the psycho-physical modelling perspective. These models were chosen because they operate under different assumptions and emphasise distinct aspects of driving behaviour. This diversity allows for a comparison of how each model responds to identical traffic scenarios, offering valuable insights into their suitability for emissions-related studies.

3.2.1. Krauss model

The Krauss model proposed by Krauss (1998) assumes that a vehicle's movement is restricted by a maximum velocity v_{max}, and that the driver selects a velocity that is not greater than the maximum safe velocity, v_{safe}. Based on these assumptions, the model describes how a following vehicle interacts with the preceding cars and how drivers attempt to avoid collisions by maintaining a distance that accounts for their speed and reaction times. Both positive and negative accelerations are considered to have a limit ($-b \leqslant \frac{\mathrm{d}v}{\mathrm{d}t} \leqslant a$, where $a > 0, b > 0$). Let the leader is at position x_l with velocity v_l, and the follower at position x_f with velocity v_f. If the length of vehicle is L, and the gap between the two vehicles is g, then the speed and position of follower vehicle after reaction time Δt can be defined as:

$$v_f(t+\Delta t) = \max\left[0, v_{des}(t) - \eta\right] \tag{2}$$

$$x_f(t+\Delta t) = x_f(t) + v_f \Delta t \tag{3}$$

Here, the desired velocity, v_{des} is formulated as:

$$v_{des}(t) = \min\left[v_{max}, v_f(t) + a\Delta t, v_{safe}(t)\right] \tag{4}$$

where, the safe velocity, v_{safe} is defined as:

$$v_{safe}(t) = v_l(t) + \frac{g(t) - g_{des}(t)}{\frac{v_l + v_f}{2b} + \tau} \tag{5}$$

In equation (5), τ ($\geqslant \Delta t$) is the reaction time of the drivers. The gap between vehicles, g and the desired gap, g_{des} can be defined as:

$$g(t) = x_l(t) - x_f(t) - L \tag{6}$$

$$g_{des} = \tau v_l \tag{7}$$

In equation (2), The random perturbation $\eta > 0$ was introduced to allow for deviations from optimal driving. In our simulation we assumed $\tau = \Delta t$. The Krauss model is often used in microscopic traffic simulations due to its simplicity and computational efficiency.

3.2.2. IDM model

The IDM proposed by Treiber *et al* (2000) is a widely used CF model that accounts for realistic driving behaviour, such as acceleration and deceleration in response to surrounding vehicles. It incorporates factors like desired speed, minimum spacing, and a time headway to model the interaction between vehicles. IDM is known for its ability to generate smooth and adaptive driving behaviours in various traffic conditions. Using IDM, the acceleration of the following vehicle $a_f(t)$ at time t can be determined using the following equation:

$$a_f(t) = a_{max}\left[1 - \left(\frac{v_f(t)}{v_{des}}\right)^{\delta} - \left(\frac{g_{des}}{g(t)}\right)^2\right] \tag{8}$$

where, a_{max} is the maximum acceleration, $v_f(t)$ is the current velocity of the following vehicle, v_{des} is the desired velocity, δ is the acceleration exponent, $g(t)$ is the actual gap between the leading and the following

vehicle, and g_{des} is the desired gap. The position of the following vehicle x_f at time $t+\Delta t$ is updated using the following kinematic equation:

$$x_f(t+\Delta t) = x_f(t) + v_f \Delta t + \frac{1}{2} a_f (\Delta t)^2 . \tag{9}$$

The gap $g(t)$ between the follower and leader is defined as in equation (6). The desired gap, g_{des} is given by:

$$g_{des} = g_0 + \max\left(v_f T + \frac{v_f(v_f - v_l))}{2\sqrt{a_{max} b}}, 0\right) \tag{10}$$

where, g_0 is the minimum gap (jam distance) when the vehicle is at a standstill, T is the desired time headway (representing the time the following vehicle wishes to maintain behind the leading vehicle), and b is the comfortable deceleration (positive value).

3.2.3. Wiedemann's model

Among other psycho-physical models, in this study we selected Wiedemann's (Wiedemann 1974) two-parameter model as it is suitable for urban, low speed movements (Durrani *et al* 2016, Farrag *et al* 2020). This model operates by defining several regimes of CF behaviour based on the relative speed and distance between vehicles. The desired distance between two stationary vehicles is given by:

$$d_0 = L + C_0. \tag{11}$$

Here, C_0 = Desired front-to-rear distance, which is parametrised as $1 + 2 \times r_{n1}$. At low speeds, the desired minimum following distance is defined as:

$$d_1 = d_0 + B. \tag{12}$$

Here, B is the speed depending term which is further parametrised as $1 + 7 \times r_{n1} \times \sqrt{v}$. In equations (11) and (12), r_{n1} is a normally distributed driver dependent parameter. The maximum following distance is expressed as:

$$d_2 = d_0 + B \times E. \tag{13}$$

In equation (13), E is parametrised as $2 - r_{n2}$. r_{n2} is also a normally distributed driver dependent parameter. Consequently, if $S_n(t)$ is the vehicle spacing between the front bumper of the leader and front bumper of follower vehicle at time t, the speed of follower vehicle can be determined by the following equation during the different phase:

$$v_f(t+\Delta t) = \min\left[\left(\frac{S_n(t) - d_0}{B}\right)^2, \left(\frac{S_n(t) - d_0}{B \times E}\right)^2, v_{max}\right]. \tag{14}$$

3.3. Selection of emissions model

Among different emissions models, the PHEM (Wyatt *et al* 2014) is one that estimates emissions based on second-by-second data on vehicle speed and acceleration. To calculate the emissions for the vehicle fleet, we used the PHEMlight emission model. PHEMlight relies on data files containing the parameters pertinent to the modelled emissions classes. The model itself was formulated through the utilisation of characteristic emission curves, delineating the emission quantity in relation to the actual engine power of the vehicle. These curves were generated through PHEM, utilising representative dynamic real-world driving cycles. Consequently, the emission and fuel consumption outputs for a vehicle during each simulation step were derived by calculating the power requisite for the vehicle

$$P_e = (P_{RR} + P_{AR} + P_{AC} + P_{RG})/\eta_{GB}. \tag{15}$$

Here,

$$P_{RR} = (m_{Vehicle} + m_{Load}) \times g \times \left(Fr_0 + Fr_1 \times v + Fr_4 + v^4\right) \times v \tag{16}$$

$$P_{AR} = (Cd \times A \times \rho/2) \times v^3 \tag{17}$$

$$P_{AC} = (m_{Vehicle} + m_{Rot} + m_{Load}) \times a \times v \tag{18}$$

$$P_{RG} = (m_{Vehicle} + m_{Load}) \times Gradient \times 0.01 \times v \tag{19}$$

$$\eta_{GB} = 0.95 \times (AE) \tag{20}$$

$***RR$ = Rolling Resistance, AR = Air Resistance, AC = Acceleration, RG = Road Gradient, GB = Gearbox, AE = Average Efficiency.

To compute the power demand, the emission factors were selected from the PHEM database, and the coefficients were determined based on the type of vehicle and engine used by the vehicles. In our simulation, we considered all vehicles to be passenger cars with a gasoline engine (EURO 4).

3.4. Design of the experiment

In our micro-simulation experiment, we coupled the selected CF models with the chosen emissions model to compare the emissions estimated by each traffic model. We used SUMO, an open source traffic simulation package (Lopez *et al* 2018), to carry out the experiment. The experiment consisted of three main phases: (1) instance selection, (2) synthetic trajectory generation for vehicle movement, and (3) traffic model calibration and emissions measurement.

(i) Instance Selection: As already noted, we focused our analysis on emissions in the neighbourhood of a primary school. Traffic network data was sourced from OpenStreetMap, with the network layout used in the experiment shown in figure 1. Signal phase descriptions and timings were retrieved from the Bradford SATURN network model (detailed signal timings are provided in supplementary documents, figure S1). The speed limit on Otley Road is 30 mph. The traffic simulation covered the period from 7:00 AM to 10:00 AM (7:00 to 8:00 warm-up period and 9:00 to 10:00 cool-down period), with school-related traffic peaking between 8:30 AM and 9:00 AM, aligning with the school gate opening from 8:45 AM to 9:00 AM. Based on the school's capacity of 220 children, the simulation assumed a maximum of 220 school-related vehicles, corresponding to each child arriving in a separate car.

(ii) Synthetic Trajectory Generation: Synthetic vehicle trajectories were generated for the period between 7:00 AM and 10:00 AM in the vicinity of the selected school, using hourly traffic flow count data. This data was obtained from the official website of the Department for Transport (2023). Vehicles were randomly generated across the time interval while adhering to traffic counts observed at specific points within the simulation area. Initially, all possible routes within the simulation area were generated using SUMO's in-built randomTrips tool. These routes were then used to generate the demand for routed vehicles, utilising the routesampler tool, which combines turn-count and edge-count data. Simulation was initially conducted using Krauss's original model, with parameters adjusted to reflect local traffic conditions. After the simulation, key information such as vehicle departure time, departure and arrival edges, and lane IDs were extracted to construct synthetic trajectories. Multiple sets of synthetic trajectories were generated for simulating scenarios involving both school and non-school traffic, as well as scenarios without school traffic. This approach enabled us to capture variations in emissions resulting from changes in the amount of school traffic.

(iii) Traffic Model Calibration and Emissions Measurement: To evaluate the performance of the selected CF models in estimating emissions, it was important to first calibrate them to a similar level. This was achieved by calibrating the IDM and Wiedemann models to produce traffic characteristics and emissions comparable to those of the Krauss model. During calibration, common parameters such as vehicle size, minimum gap between leader and follower, maximum acceleration, and deceleration rates were kept consistent across all models. Only the model-specific parameters were adjusted to match the emissions or traffic characteristics produced by the Krauss model. Table 1 provides the common and model-specific parameters for the three selected CF models. These parameter values imposed additional constraints on the speed optimisation model. For example, the maximum allowable acceleration and deceleration rate for a passenger car was assumed to be 2.6 m s^{-2} and 4.5 m s^{-2} respectively. In this study, we focused on comparing PM_x emissions, though similar methodologies could be applied to other vehicular pollutants. The emissions measurement experiment included three main scenarios: (1) Single follower-leader scenario, (2) Steady-state condition with school and non-school traffic flow, and (3) Changing school traffic flow. Various metrics such as average speed and emissions levels were used to evaluate the models under the different scenarios. The details of the scenarios and metrics used to compare the models are listed in table 2.

3.5. Emissions reduction strategy: speed limit optimisation

The optimal speed limit, in the context of this study, was defined as the speed limit that minimises total vehicle emissions around the school area during the main hour of the morning school commute (8:00 AM to 9:00 AM). The speed limit was adjusted only on roads in front of the school gate, where school children commonly walk to school between 8:00 and 9:00 (figure 1). For each CF model, we compared the objective function representing the relationship between PM_x emissions and speed limits to evaluate the models' sensitivity in providing optimal speed limit solutions.

The simulation models were tested under a defined range of potential speed limits, from 3 m s^{-1} to 20 m s^{-1}. The speed limit directly affects the parameters of the CF models. It sets the value of v_{max} and,

Table 1. Parameters used for traffic simulation (* These are the values at which the models were able to closely approximate vehicular flow).

Traffic model	Parameter	Values
All selected traffic model	Length of vehicle (m)	5
	Minimum gap (m)	2.5
	Maximum speed limit ($m\,s^{-1}$)	70
	Vehicle class	Passenger
	Acceleration ($m\,s^{-2}$)	2.6
	Deceleration ($m\,s^{-2}$)	4.5
	Emergency deceleration ($m\,s^{-2}$)	9
	Driver's desired time headway (τ)	1
	Emission class	*PC_G_EU4*
	Deviation of the speed factor	0.1
Krauss model	The frequency for updating the acceleration associated with driver imperfection	1
	Sigma	0.5
IDM model	Acceleration exponent (δ)	1–5 (5*)
	Internal step length	1
Wiedemann model	Desire for security (r_{n1})	0.1–1 (0.1*)
	Accuracy of situation estimation (r_{n2})	0.5–1 (1*)

Table 2. Scenario description and metrics used to evaluate and compare the models.

Scenario ID	Scenario description	Metrics used for comparison
1	Single follower-leader scenario	Total travel time (s) Total waiting time (s) Avg. speed ($m\,s^{-1}$) Avg. acceleration ($m\,s^{-2}$) Avg. deceleration ($m\,s^{-2}$) Total PM_x(mg)
2	Steady-state condition with school and non-school traffic flow	Flow-density relation Speed-density relation Average speed ($m\,s^{-1}$) Total and average fuel consumption (g) Total and average PM_x ($mg\,g^{-1}$) emissions
3	Changing school traffic flow scenario	Traffic flow Total and average fuel consumption (g) Total and average PM_x ($mg\,g^{-1}$) emissions

depending on the model, influences the desired velocity/acceleration of both the leading vehicle and the followers. For example, in the Krauss and Wiedemann model, the influence of v_{max} is reflected in determining the velocity of the vehicle (equations (4) and (14)). In contrast, for the IDM model, the influence of v_{max} is reflected through its effect on the desired velocity, which directly controls the acceleration (equation (8)). Additionally, we assessed the impact of varying speed limit precision on emissions estimation. Speed precision was allowed to vary across different increments $-1\,m\,s^{-1}$, $0.5\,m\,s^{-1}$, and $0.1\,m\,s^{-1}$—to investigate whether greater precision leads to different objective functions and optimisation solutions.

4. Results

This section presents the results of the comparative analysis of selected CF models, highlighting emissions measurements and identifying optimal solutions for emissions reduction. For clarity, the findings are organised into two subsections: (1) a comparison of emissions calculated using the selected CF models, and (2) a sensitivity analysis of optimal speed limits to minimise emissions.

Table 3. One single leader's and follower's trajectory profile and performance on emissions measurement across different CF models (total trajectory length: 952 m).

Attributes	Krauss model		IDM model		Wiedemann model	
	Leader	Follower	Leader	Follower	Leader	Follower
Total travel time (sec)	131	133	131	133	131	134
Total waiting time (sec)	34	36	38	27	52	10
Avg. speed ($m\,s^{-1}$)	7.25 ± 5.56	7.19 ± 5.28	7.22 ± 6.11	7.15 ± 5.19	7.25 ± 6.59	7.12 ± 5.24
Avg. acceleration ($m\,s^{-2}$)	1.07 ± 0.80	1.01 ± 0.82	1.29 ± 1.02	0.87 ± 0.97	2.34 ± 0.55	1.84 ± 0.99
Avg. deceleration ($m\,s^{-2}$)	1.15 ± 1.32	0.98 ± 1.15	1.14 ± 0.78	0.89 ± 0.86	3.11 ± 2.04	1.05 ± 1.42
Total fuel consumption (g)	105.65	99.06	96.82	100.925	108.13	113.32
Total PM_x (mg)	7.245	5.976	6.83	5.27	11.99	12.56

4.1. Emissions measurement

Since emissions measurements directly influence the emissions minimisation problem, the comparison process progressively examines the differences among the three models: (1) single follower-leader pairs, (2) model differences under steady-state conditions involving both school and non-school traffic, and (3) the impact of varying school traffic flow on emissions.

4.1.1. Single follower-leader scenario

To compare the performance of each selected CF model in a single follower-leader scenario, we allowed one follower vehicle to complete a test scenario, specifically traversing from one edge to the other of the school instance, in response to the leader vehicle's trajectory. The length of the trajectory was 952 meters. The CF model parameters used in this scenario were identical to those applied in the scenario with a vehicle fleet (scenario 2). For the IDM model, the parameters were set to $\delta = 5$, and $Stepping = 1$, while for the Wiedemann model, $r_{n1} = 0.1$, $r_{n2} = 1$. These settings successfully replicated the vehicular flow of a fleet produced by the Krauss model.

A summary of the output from this single follower-leader scenario is presented in table 3 and supplementary figure S2. Although the primary focus of this article was on emissions measurement, we also compared other attributes such as travel time, waiting time, average speed, and acceleration/deceleration indices, as these factors are directly linked to emissions. Table 3 shows that the travel times for both the leader and follower vehicles to complete their journeys were approximately the same across different models. The waiting times for the follower and leader vehicles varied across the models. Waiting time was defined as the duration during which a vehicle was either stationary or moving at a speed of less than $0.1\ m\,s^{-1}$. The difference between the waiting times of the follower and leader was the lowest in the Krauss and IDM model, while it was the highest in the Wiedemann model.

Similar to the travel times, the average speeds of both the follower and leader vehicles, along with their respective deviations from the mean, exhibited comparable patterns. However, the Wiedemann model showed higher average acceleration for the leader, while the Krauss model exhibited the lowest average acceleration for the leader. The highest average acceleration for the follower was also observed in the Wiedemann model. Notably, the IDM model had the highest standard deviation in mean acceleration compared to both the Krauss and Wiedemann models. In terms of deceleration, the Wiedemann model showed the highest average deceleration and the greatest dispersion from the mean for both the leader and follower. As with the other attributes, discrepancies across the models were also observed when comparing the total fuel consumption of the follower and leader during their journey. The Wiedemann model demonstrated the highest fuel consumption and total PM_x emissions for both the leader and follower. In contrast, the IDM model exhibited the lowest fuel consumption for the leader and the lowest total PM_x for both the leader and follower. However, the Krauss model recorded the lowest overall fuel consumption, with total emissions falling between those of the Wiedemann and IDM models. These results underscore the nonlinear relationship between fuel consumption and PM_x emissions across the models.

4.1.2. Steady-state scenario

To compare the models under steady-state conditions, our simulation included both school and non-school traffic. For the school traffic, a worst-case scenario was assumed where all children ($n = 220$) were driven to school, with each child arriving in a separate car.

The number of vehicles traversing the simulation area between 7:00 AM and 10:00 AM is shown in figure 2(a). During the target period (8:00-9:00 AM) the number of vehicles in the simulation area followed a similar trend across all models. The largest differences between the models occurred during the warm-up and cool-down periods. During the target period, while the IDM and Wiedemann models showed slight

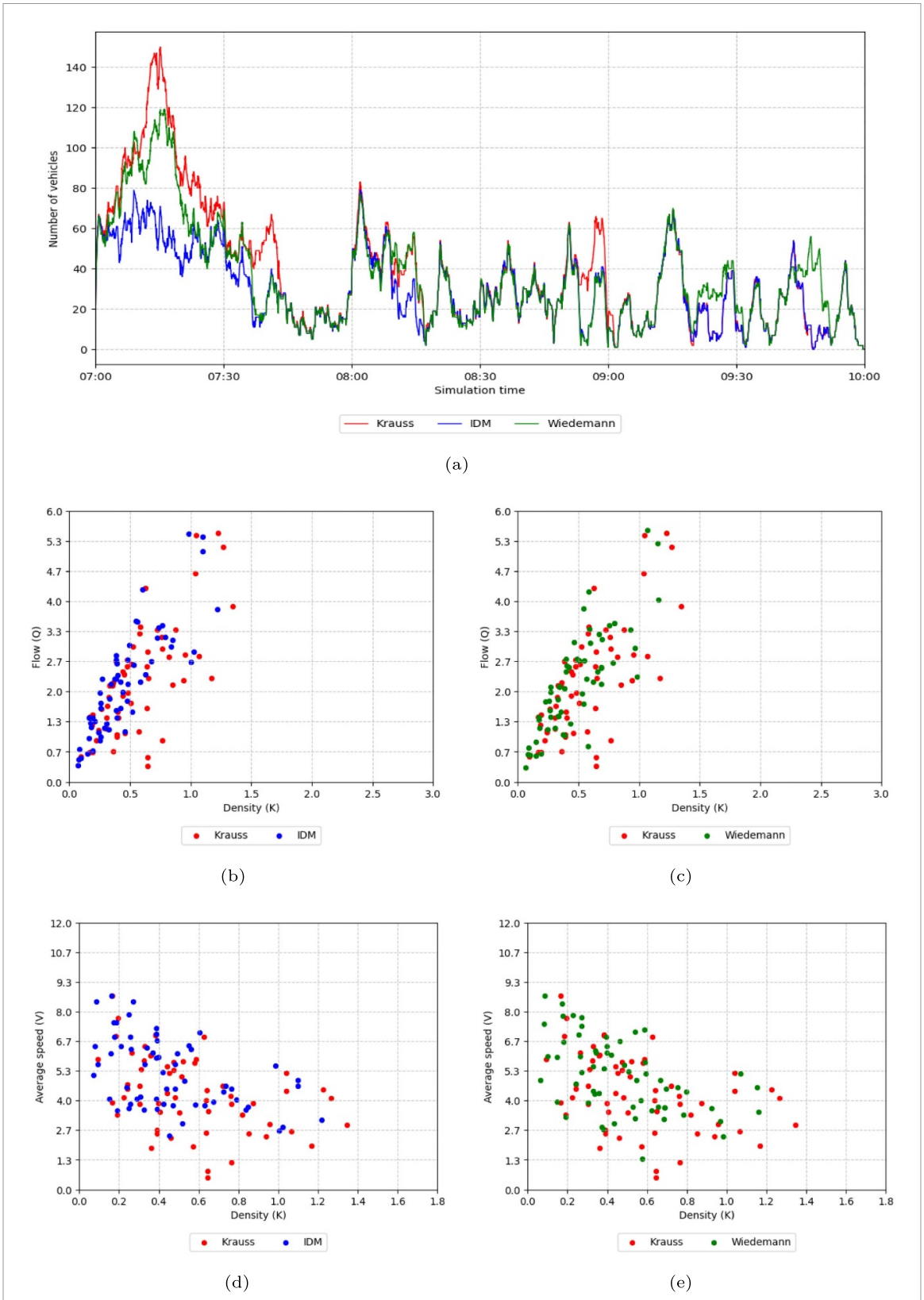

Figure 2. Differences across models in steady-state conditions (a) Number of vehicles traversing during the simulation time (7:00 to 10:00); For the school time (8:00 to 9:00): (b) Flow (Q) - density (K) relationship between Krauss and IDM model, (c) Flow (Q) - density (K) relationship between krauss and Wiedemann model, (d) Speed (V) - Density (K) relationship between Krauss and IDM model, (e) Speed (V) - Density (K) relationship between Krauss and Wiedemann model.

variations compared to the Krauss model, overall the selected CF models exhibited very similar vehicular flow patterns.

When comparing the fundamental relationships across the models, no discernible differences were observed between the IDM and Wiedemann models during the 8:00 AM to 9:00 AM period. The IDM and

Table 4. Average speed, fuel consumption and emissions (at each time-step 1 s) profile of the entire fleet between 8:00 to 9:00.

Parameters	Krauss model	IDM model	Wiedemann model
Avg. speed	4.37 ± 2.38	5.12 ± 2.36	4.95 ± 2.46
Avg. fuel consumption (g) per vehicle	21.01 ± 12.39	20.14 ± 12.73	19.82 ± 12.96
Avg. PM_x emissions (mg) per vehicle	1.38 ± 1.24	1.32 ± 1.16	2.14 ± 1.87

Wiedemann models adhered to the same macroscopic fundamental diagram (MFD). For instance, the average flow-density relationships between IDM and Krauss, as well as Wiedemann and Krauss models, followed a nearly identical distribution (figure 2(b)), exhibiting similar maximum average flow and critical density values. Additionally, the Wiedemann and IDM models displayed a comparable distribution of observations beyond the critical density. However, while the Wiedemann and IDM models showed flow patterns similar to the Krauss model, the flow-density relationship revealed that the Krauss model had a greater number of observations beyond the critical density compared to the other two models.

Similarly, the average speed-density relationships revealed only subtle differences across the models. Compared to the Krauss and Wiedemann models, the IDM model exhibited relatively higher speed variation at lower densities. In contrast, the Wiedemann model displayed a steeper speed-density relationship than both the Krauss and IDM models, highlighting a more pronounced decrease in speed with increasing density. This suggests that the Krauss model demonstrated a more gradual reduction in speed in response to rising density (figure 2(d)). Furthermore, the scattered distribution in the speed-density plots suggested that the Krauss model exhibited greater variability in speed at a given density compared to the IDM and Wiedemann models.

In addition to comparing the fundamental relationships across the different CF models, we also analysed the average speed profile, total fuel consumption (g), and total PM_x emissions (mg) at each time step, as well as the moving average over consecutive 100-second intervals, focusing on the 8:00 AM to 9:00 AM period. In figures 3(a)–(i), the average speed, total values of fuel consumption and total values of PM_x emissions at each time step are represented by the grey points, while the smoothed moving average trend over 100-second intervals is shown by the coloured solid line. Different colours (red, blue, and green) were used to highlight the moving average trend across different CF models. Moreover, the summary statistics of the entire fleet are also shown in table 4.

When comparing the average speed per vehicle at each time step (figures 3(a)–(c)), the IDM and Wiedemann models displayed an increasing trend, whereas the Krauss model exhibited relatively flat trends. The IDM model's average speed at each time step ranged from 2.9 m s^{-1} to 8 m s^{-1}, showing less pronounced fluctuations compared to the Krauss and Wiedemann models. Additionally, both the Wiedemann and Krauss models experienced occasional drops in speed, often falling below 2 m s^{-1}. For the entire fleet, the average speed at each time step and its dispersion from the mean were similar across the selected models, while the IDM model demonstrated a relatively higher average speed and lower dispersion (table 4). This is consistent with the moving average speed profiles, where the IDM model showed less fluctuation in speed compared to the Krauss and Wiedemann models (figures 3(a)–(c)), resulting in a higher mean and lower speed variability for the entire fleet. As with the single follower-leader scenario, the average speed at each time step did not exhibit appreciable discrepancies between the models (table 4). However, the moving average speed profiles (figures 3(a)–(c)) revealed substantial differences at the micro level. For example, the lowest average speed per vehicle in the Krauss model occurred after 8:50 AM, whereas for the Wiedemann model, it occurred before 8:20 AM.

Unlike the speed profiles, the total fuel consumption profiles shown in figures 3(d)–(f) displayed a decreasing trend between 8:00 AM and 9:00 AM across all models. This result is plausible, as an increase in speed typically leads to more efficient fuel combustion, resulting in lower fuel consumption. Although the moving averages of total fuel consumption revealed differences between the models, these differences were less pronounced compared to other attributes such as speed and emissions. Summary statistics of fuel consumption indicated that the Wiedemann model had the lowest average fuel consumption per vehicle but exhibited the highest variation from the mean compared to the IDM and Krauss models (table 4). As shown in the moving average plot (figure 3(f)), the Wiedemann model exhibited a wider variation in fuel consumption values across time, resulting in a moving average trend that appeared less consistent compared to the other models. In contrast, the Krauss model demonstrated the highest average fuel consumption and the least variation from the mean for the entire vehicle fleet between 8:00 AM and 9:00 AM (table 4). This contrasts with observations from the single follower-leader scenario, where the IDM and krauss model consistently showed better fuel efficiency with minimal fluctuation.

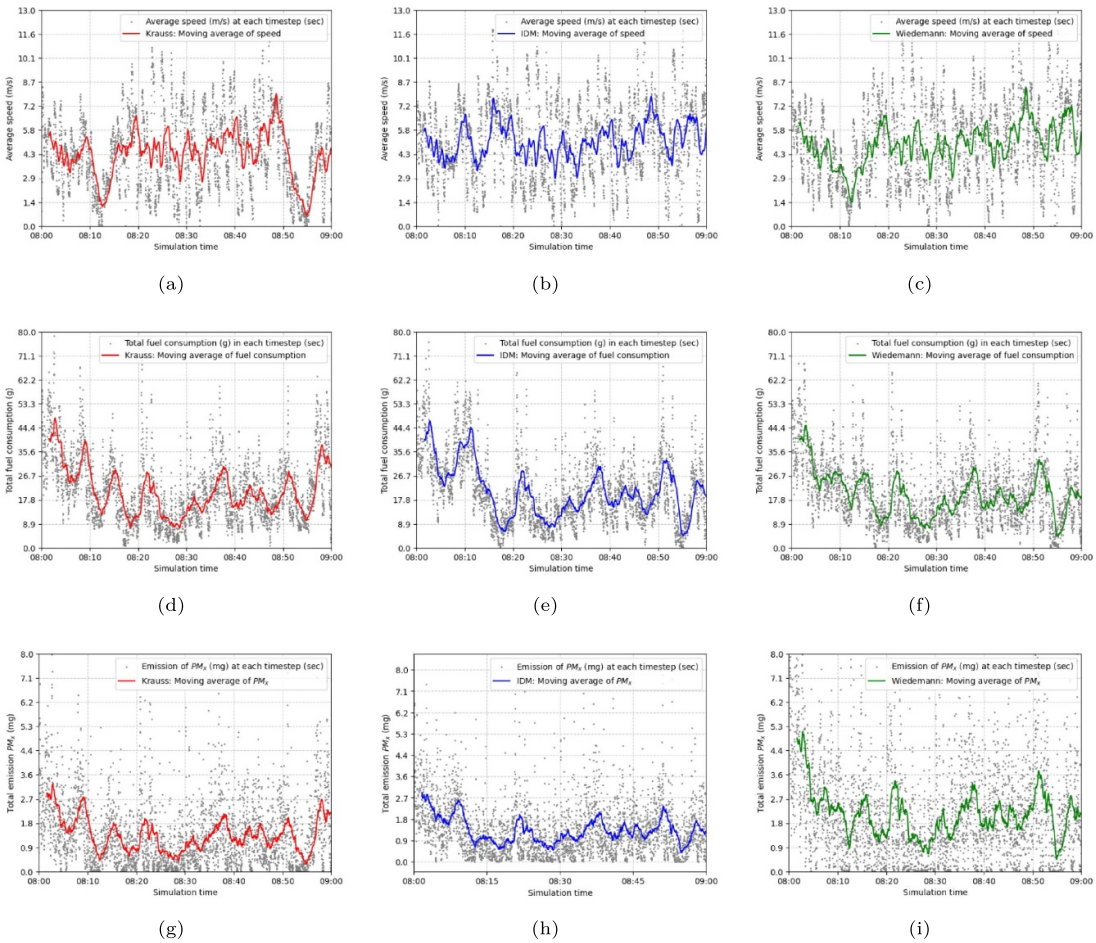

Figure 3. Differences across models in steady-state conditions: (a)–(c) - Average speed at each time step, (d)–(f) - Total fuel consumption at each time step and average fuel consumption over 100-second intervals, (g)–(i) - Total PM_x emissions at each time step and average PM_x emissions over 100 s intervals.

In terms of PM_x emissions, the IDM model exhibited lower emissions at each time step, with less variation from the mean trend (figure 3(h)). Conversely, the moving average profile shown in figure 3(i) and the summary statistics in table 4 revealed that the Wiedemann model had the highest emissions, followed by the Krauss model and then the IDM model. Additionally, compared to the IDM model, the Wiedemann model and, to a lesser extent, the Krauss model demonstrated greater variability, characterised by frequent and sharp changes in emissions.

4.1.3. Changing school traffic flow scenario

To compare the models in terms of emissions measurement, we also examined a scenario with varying traffic flow conditions, by varying the number of school cars from 0 to 220. In the initial iteration, all of the school children ($n = 220$) were driven to school. Then, a small number ($m = 2$) of children who had previously been driven to school were assumed to switched to a non-motorised mode (such as walking/cycling), and this process continues, through $n, n-m, n-2m, \ldots$ until no children were driven. The reason to follow this approach was in order to minimise Monte Carlo noise in comparisons across different scenarios, and in particular, noise caused by the random departure times at which vehicles were generated. By first generating departure times for the maximum pool of n potential vehicles, m vehicles are then randomly chosen for deletion and the pool reduced to $n-m$, importantly with the remaining vehicles maintaining the same departure times they were assigned in the scenario with n vehicles, and this process continues with the next step deleting a further m vehicles from the remaining pool of $n-m$. This process allows us to better exemplify systematic patterns in the model results.

Figures 4(a) and (b) illustrate the pattern of vehicular flow under different school traffic conditions. These figures show that for each traffic model there was no unique set of parameters able to replicate the vehicular flow. In some cases, different parameter values for each model can produce similar flow patterns, but distinct differences still exist between the models. For instance, while different δ parameters of the IDM

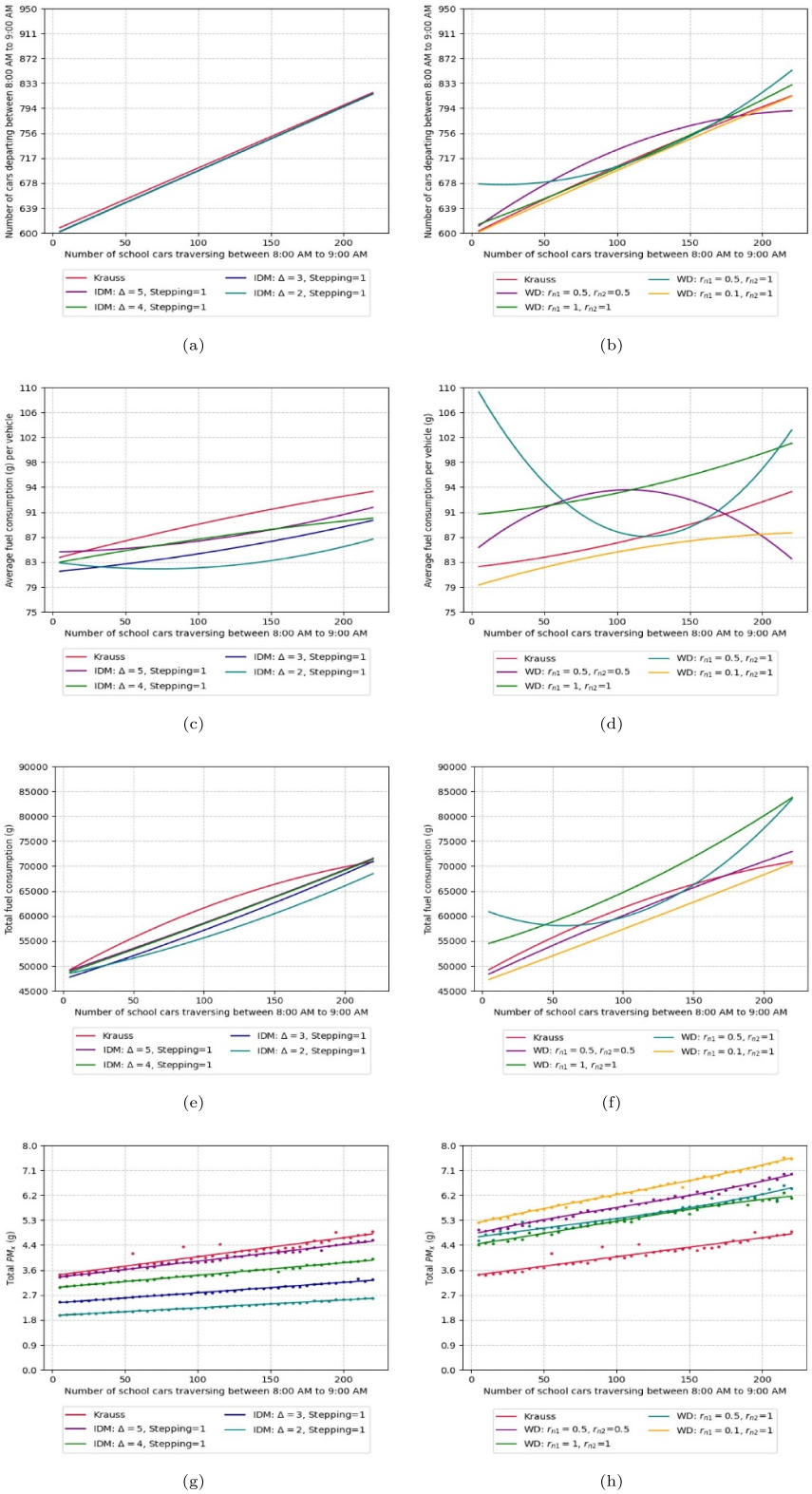

Figure 4. Changing school traffic scenario: (a), (b) - Number of cars traversing between school time, (c), (d) - Average fuel consumption per vehicle, (e), (f) - Total fuel consumption, (g), (h) - Total PM_x emission.

model can approximate the flow of the Krauss model, varying r_{n1} and r_{n2} parameter values in the Wiedemann model results in noticeably different vehicular flow patterns. At changing school traffic conditions, figures 4(c) and (d) display the differences in average fuel consumption, while figures 4(e) and (f) show the total fuel consumption across traffic models for different calibrated parameters. These figures emphasise that although certain parameters can closely replicate vehicular flow, there were substantial differences in both average and total fuel consumption. Parameters that yield the closest match to vehicular

flow-such as $\delta = 5$, $Stepping = 1$ for IDM, and $r_{n1} = 0.1$, $r_{n2} = 1$ for Wiedemann-align with the Krauss model's average and total fuel consumption, showing the lowest deviation from it. The total PM_x emissions are shown in figures 4(g) and (h), which indicated that parameters that closely replicate vehicular flow and fuel consumption also recover PM_x emissions with relatively low error compared to the Krauss model for the IDM model. The error was lowest under low traffic flow conditions, such as when there was no school traffic, but it began to increase as the number of school traffic increased. However, this is not the case for the Wiedemann model. The parameters that minimise error in the Wiedemann model's emissions outputs ($r_{n1} = 1$, $r_{n2} = 1$) still show substantial discrepancies in fuel consumption and vehicular flow recovery. However, in both cases-whether replicating the vehicular flow or estimating emissions-the Wiedemann model's measured PM_x emissions were approximately double those of the Krauss and IDM models. It is noteworthy that to achieve similar emissions levels from the vehicle fleet under specific school traffic conditions, a relatively higher stepping parameter value of 1 was adopted for the IDM model. While this value is considered relatively unsafe for the IDM model, it was used to facilitate a fair comparison of model performances under comparable emissions outputs. With a smaller stepping parameter, the IDM model could not replicate emissions comparable to those of the Krauss model.

4.2. Optimal speed limit

To test the sensitivity of optimal solutions across different CF models, we analysed the impact of speed limits as a control measure to reduce emissions in a school zone. Figure 5 shows the total PM_x emissions (g) for the three different CF models tested across a range of pre-defined speed limits with an increment of 1 m s^{-1} (figure 5(a)), 0.5 m s^{-1} (figure 5(b)), and 0.1 m s^{-1} (figure 5(c)).

These tests revealed that the same speed limit could influence model-specific variables such as speed and acceleration in different ways, leading to different emissions profile. In other words, the formulation of speed and acceleration in CF models substantially influenced the optimisation objective function. For example, IDM adjusts acceleration dynamically based on leader-follower gaps, while Wiedemann incorporates psychophysical thresholds, and Krauss relies on safe distance calculations. Due to these differences and all else being equal, the impact of the speed limit on emissions was found to be not uniform across the models. Instead, the results highlighted the sensitivity of the objective function to the underlying behavioural assumptions in each traffic model.

In figures 5(a)–(c), the Krauss and Wiedemann models exhibited a relatively flat emissions profile at lower speed limits. For the Krauss model, this flat trend persisted up to a speed limit of 14 m s^{-1}, while for the Wiedemann model, it was up to 11 m s^{-1}. After these thresholds, emissions increased dramatically with augmenting speed limits. On the other hand, the IDM model showed a consistent decrease in emissions as the speed limit increased from 3 m s^{-1} to around 11 m s^{-1}, with emissions gradually increasing afterward. IDM employs dynamic modelling of acceleration and deceleration, emphasising speed adjustments based on the gap between the follower and leader (see equations (5)–(8)). This captures reactive behaviours, such as realistic stop-and-go traffic. As a result, IDM exhibited a relatively smooth, concave emission curve under different speed limit conditions. Across all scenarios, the IDM model consistently demonstrated the lowest emissions compared to the other two models for a speed limit above 8 m s^{-1}. In contrast, the Krauss model bases the velocity and acceleration of the follower on those of the leader, while maintaining a safe distance. In congested urban areas, where lower speed limits are typical, the follower's velocity is generally constrained by the leader's speed and safety distance, with limited opportunity to accelerate or adjust speed. This resulted in relatively stable emissions at lower speed limits. However, as the speed limit increased, the Krauss model allowed for greater acceleration and speed changes, leading to a substantial rise in emissions. Between speed limits of 8 m s^{-1} and 14 m s^{-1}, emissions from the IDM and Krauss models showed minimal differences, but for speed limits below 8 m s^{-1} or above 14 m s^{-1}, the variation between these models became more pronounced.

The Wiedemann model, on the other hand, consistently exhibited higher PM_x emissions compared to both Krauss and IDM across all speed limits. This behaviour is attributed to its oscillatory nature, driven by frequent transitions between driving zones (e.g. following and approaching states) based on headway distance and relative speed. These micro-accelerations and decelerations result in increased emissions, particularly at lower to moderate speeds. As the speed limits was increased beyond 15 m s^{-1}, emissions from the Wiedemann model increased sharply. This can be attributed to more aggressive braking and acceleration events as drivers transition between behavioural states. Such aggressive acceleration and deceleration were also observed in single follower-leader scenarios. In that case, due to the reduced number of vehicles, both the leader and the follower were more likely to operate at or near their desired velocities, leading to pronounced speed adjustments. The steep rise in emissions at higher speed limits reflects Wiedemann's emphasis on a driver's perception and reaction over smooth traffic flow, making it more sensitive to abrupt

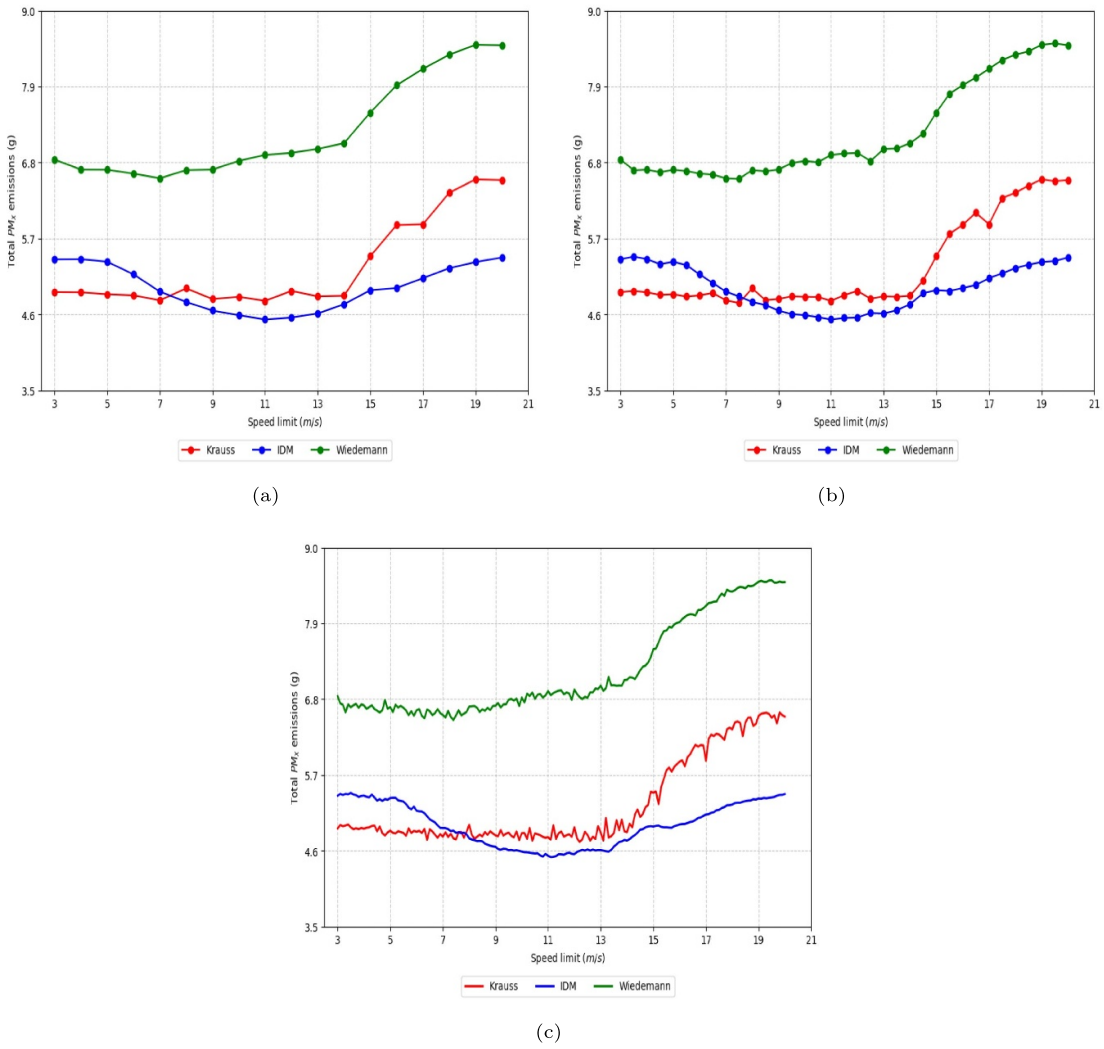

Figure 5. Total PM_x emissions across a range of speed limit for three selected CF models (a) standard precision with a 1 increment, (b) moderate precision with a 0.5 increment, (c) high precision with a 0.1 increment.

changes in headway and relative speeds. Consequently, we may expect the Wiedemann model to predict relatively high emissions levels in higher-speed scenarios, compared with other approaches.

When comparing the objective function of the selected optimisation problem at different precision levels of the decision variable (speed limit), emissions exhibited distinct behaviours across the CF models. In the standard precision scenario (figure 5(a)), the emissions exhibited minor variations across smaller differences in speed limits, such as between 4 m s^{-1} and 5 m s^{-1}. However, in the high-precision scenario (figure 5(c)), emissions displayed greater variability, highlighting the models' sensitivity to changes in speed limit. For instance, in the highest precision scenario (figure 5(c)), the IDM model captured finer fluctuations in emissions while also maintaining the continuity in the objective function. This reflects IDM's capacity to dynamically model acceleration and deceleration based on the gap between the follower and leader, which helps minimise unnecessary accelerations, especially at lower speeds. In contrast, the Wiedemann model exhibited greater fluctuations in emissions in the speed range between 3 m s^{-1} and 7 m s^{-1}, indicating higher sensitivity to minor speed variations at lower speed limits. This behaviour can be attributed to its psychophysical thresholds and oscillatory nature, which lead to frequent transitions between driving states, such as 'following' and 'approaching'. Additionally, the Krauss model showed mentionable fluctuations in emissions at higher precision levels within the speed range of 13 m s^{-1} to 15 m s^{-1}. This could be due to its reliance on maintaining safe distances between vehicles, which results in more pronounced accelerations and decelerations when the follower adjusts to the leader's behaviour in response to higher speed limits.

One important reason for examining the sensitivity of precision is that, depending on the level of precision, the objective function may shift from a continuously differentiable curve to one with discontinuities as observed for Krauss and Widemann model. This shift can significantly influence the choice of optimisation methods used to find the optimum solution. For instance, with the IDM model, the

continuous nature of its objective function appears to allow for the use of gradient-based optimisation methods to efficiently identify optimal results. However, at higher precision levels, the Krauss and Wiedemann models may exhibit more irregularities or discontinuities in their objective functions due to their dependence on extremely reactive driving behaviours, such as sudden accelerations and decelerations. In such cases, optimisation approaches like gradient descent may become ineffective, as these methods are prone to getting stuck in local optima. For these models, alternative techniques, such as the cross-entropy method or meta-heuristic algorithms (e.g. genetic algorithm, simulated annealing, or particle swarm optimization), may be more suitable to navigate the complex solution landscape and avoid convergence to suboptimal results.

5. Discussion

The coupling of microscopic traffic simulation models with emissions models offers a powerful tool for assessing and optimising traffic control strategies to reduce fuel consumption and vehicle emissions. Although many studies use traffic simulation for emissions analysis and designing traffic calming measures, most focus on calibrating a selected traffic model to replicate observed traffic flow, limiting their investigation. This approach creates a gap in the literature and raises the question: Are optimal emissions control strategies appropriately tailored to account for the sensitivity of traffic models in capturing vehicle dynamics and emissions? To address this gap, we compared three CF models, each developed within distinct theoretical frameworks, and evaluated their performance using both trip-based and emission-specific metrics. This analysis aimed to assess their sensitivity in designing an effective traffic control strategy to reduce emissions around a school zone case study. For emissions analysis, scenarios ranged from single follower-leader interactions to varying school traffic conditions. Finally, we tested these models' effectiveness in designing a traffic control strategy to reduce emissions by imposing speed limits around the school area.

Under the single follower-leader CF scenario, the results from the comparative analysis showed that the models exhibited subtle differences in macroscopic traffic attributes. When comparing travel time and average speed of the follower and leader, the variation across models was minimal. Similarly, when examining the average speed of the entire fleet, differences across models were only noticeable when analysing the average speed at each time step and the corresponding moving average over a certain time period. In fact, vehicular flow during the school time was nearly identical across the models. Additionally, the MFD further supported the idea that each model accurately represented the same traffic scenario, indicating consistency in their ability to replicate aggregated traffic characteristics such as flow, density, and average speed. These findings suggested that when the key indicators were travel time or average speed, all three models could predict similar vehicular movements. It was also evident in other traffic modelling studies that microscopic traffic models with different driver behaviours can lead to similar macroscopic traffic dynamics (Klar and Wegener 2000, Treiber *et al* 2006, Chevalier *et al* 2015). However, when examining more microscopic traffic attributes, such as the acceleration and deceleration of the follower and leader or the entire fleet, notable differences were observed in our study (consistent with the findings of the study of Pourabdollah *et al* (2017) for different vehicular platoons). For instance, in our study, the Wiedemann model exhibited higher average acceleration and deceleration values, leading to higher emissions, as shown by the emissions output of PM_x in the analysis. In contrast, the Krauss and IDM models displayed less variation in acceleration, resulting in lower emissions. These findings highlighted that when coupling traffic simulation with emissions models and measuring emissions based on average speed, vehicular flow, or other macroscopic attributes, the differences across models could be subtle, and emissions measurements could be inaccurate. Hence, for urban area modelling, where frequent stop-and-go traffic is common, traffic models need to be sensitive enough to capture acceleration and deceleration patterns, while emissions models must be responsive to micro-level traffic dynamics.

Moreover, the results from the three scenarios suggested that replicating similar vehicular flow and average speed could still produce different emissions outcomes, indicating a need to reconsider the focus of traffic model calibration. The findings suggested that differences in fuel consumption and emissions estimates might arise from how each CF model captures vehicle dynamics such as acceleration and deceleration. In this study, the Wiedemann model showed relatively higher average acceleration and deceleration with greater variability, leading to higher calculated emissions. Interestingly, it also exhibited lower average fuel consumption than other models. While this divergence did not imply over- or underestimation in the absence of empirical validation, it highlighted how model characteristics could influence measured outcomes and the importance of model selection in emissions and fuel consumption studies. Traditionally, CF models have been calibrated with an emphasis on replicating traffic flow patterns. However, results from our study revealed that such calibration might result in models that accurately reflect traffic flow but misrepresent fuel consumption and emissions. A review based study by Madziel (2023) also

emphasised that users of simulation models rely on parameters such as traffic volume calibration to ensure that the simulation closely reflects reality, which is inefficient in terms of vehicle emissions. Hence, given the growing importance of reducing emissions in urban environments, calibrating models based solely on traffic flow metrics could lead to sub-optimal emissions reduction strategies. Instead, the findings suggested that calibration should prioritise emissions accuracy, ensuring the model accurately captures the relationship between driving behaviour, fuel use, and emissions. Shifting the focus toward emissions calibration would enable the development of more effective traffic management strategies that optimise both vehicular movement and environmental impact.

Furthermore, the study results highlighted that the objective function for minimising emissions through speed limit optimisation was not consistent across different CF models. Each model's response to changes in speed limits and sensitivity to precision demonstrated distinct emissions patterns. These results highlighted the complexities of emissions minimisation, such as selecting the appropriate traffic model to estimate emissions, the impact of decision variables on traffic dynamics that might lead to emissions, optimisation methods, managing Monte Carlo simulation noise, and addressing potential specification and computational errors. For example, our study findings showed that the simplicity of the Krauss model, which represents vehicle responses to acceleration or deceleration based on safety distance, seemed to make it less effective in capturing the influence of speed limits on emissions measurements. This is particularly relevant in local areas where speed limits are typically low, as the model's assumptions may not fully reflect the dynamics that influence emissions in such conditions. Furthermore, variations in the precision of decision variables could impact the accuracy of the optimisation model, suggesting the need for careful model constraints to mitigate such challenges and ensure reliable optimisation outcomes. For example, in our case study the IDM model suggested an optimal speed limit of approximately 11 $\mathrm{m\,s^{-1}}$, and this could be determined at different levels of precision of the decision variable. The Wiedemann model, on the other hand, suggested 7 $\mathrm{m\,s^{-1}}$ as the optimal solution when considering a low precision objective function, whereas at higher precision the solution was less clear due to the variability in the objective function. These features implied that care is needed in the selection of appropriate optimisation algorithms, depending on the choice of traffic model, to avoid being trapped in suboptimal solutions.

6. Further research

To reduce the environmental impact of traffic and mitigate the financial losses caused by congestion, efforts have been made to understand traffic flow dynamics and develop strategies for controlling and optimising it. In this study, we experimentally evaluated and analysed the sensitivity of different CF models in measuring emissions and designing optimal traffic control measures aimed at emissions reduction. Although this research explored the sensitivity of these models in an optimisation problem through an experimental setup, there is significant scope for future investigation.

Future research could involve the use of real-world traffic data and pollutant counters to validate the findings obtained from the experiment carried out in this study. Field-level observations would help distinguish which models are better suited for accurately measuring emissions, whether by replicating traffic flow or directly capturing emissions outputs. Such studies are particularly important in areas with a large number of active population (e.g. downtown regions), for understanding prolonged exposure to emissions among those who spend more time on the road, such as pedestrians and lower-income commuters. Conducting similar comparative assessments in these contexts would support more accurate risk assessment and ensure that emissions mitigation strategies are not overly dependent on a single CF model, which may not reflect the full range of real-world local traffic conditions. Additionally, this study focused on traffic flows consisting of a single type of vehicle. Future research could expand to consider mixed traffic conditions, evaluating how various CF models perform in measuring emissions and designing emission-reduction strategies in such scenarios. Moreover, field-based studies could also help identify external factors like weather, wind speed, and land-use patterns, and their contributions to emissions. While we investigated the differences in identifying optimal speed limits, future studies could apply similar comparisons to optimise traffic signals. Ultimately, our intention is that this study opens new pathways in emissions research by encouraging the calibration of traffic models specifically to improve emissions measurement and optimisation.

Data availability statement

The data that support the findings of this study are openly available at the following URL/DOI: https://roadtraffic.dft.gov.uk/local-authorities/195 (Department for Transport 2023).

Acknowledgment

This study was conducted as part of the OptiWaSP—Optimised Walking Schoolbus Planning project (Grant Number: 121566) financed by Engineering and Physical Sciences Research Council (EPSRC). We acknowledge the data support from the Bradford City Council.

Conflict of interest

The authors declare that they have no known competing financial or personal relationships that could have appeared to influence the work reported in this paper.

Author contributions

Khatun E Zannat 0000-0003-3108-5732
Conceptualization (lead), Data curation (lead), Formal analysis (lead), Investigation (equal), Methodology (equal), Resources (equal), Software (lead), Validation (equal), Visualization (lead), Writing – original draft (lead), Writing – review & editing (equal)

Judith Y T Wang 0000-0002-3361-6413
Funding acquisition (supporting), Investigation (equal), Methodology (equal), Resources (equal), Validation (equal), Writing – review & editing (equal)

David P Watling 0000-0002-6193-9121
Funding acquisition (lead), Investigation (equal), Methodology (equal), Resources (equal), Validation (equal), Writing – review & editing (equal)

References

Abdull N, Yoneda M and Shimada Y 2020 Traffic characteristics and pollutant emission from road transport in urban area *Air Qual. Atmos. Health* **13** 731–8

Abudayyeh D, Nicholson A and Ngoduy D 2021 Traffic signal optimisation in disrupted networks, to improve resilience and sustainability *Travel Behav. Soc.* **22** 117–28

Ajayi S A, Adams C A, Dumedah G and Adebanji A O 2024 The impact of vehicle engine characteristics on vehicle exhaust emissions for transport modes in lagos city *Urban Plan. Transp. Res.* **12** 2319328

Ali M, Kamal M D, Tahir A and Atif S 2021 Fuel consumption monitoring through copert model-a case study for urban sustainability *Sustainability* **13** 11614

Alshayeb S, Stevanovic A, Mitrovic N and Espino E 2022 Traffic signal optimization to improve sustainability: a literature review *Energies* **15** 8452

André M 2004 The artemis european driving cycles for measuring car pollutant emissions *Sci. Total Environ.* **334** 73–84

Aw A and Rascle M 2000 Resurrection of "second order" models of traffic flow *SIAM J. Appl. Math.* **60** 916–38

Bai S, Eisinger D and Niemeier D 2009 MOVES vs. EMFAC: a comparison of greenhouse gas emissions using los angeles county *Transportation Research Board 88th Annual Meeting, paper* (*Washington DC, United States, 2009*) pp 09–0692

Bando M, Hasebe K, Nakayama A, Shibata A and Sugiyama Y 1995 Dynamical model of traffic congestion and numerical simulation *Phys. Rev. E* **51** 1035

Cameron M 2022 Economic analysis of optimum speeds on rural state highways in new zealand *Technical Report* New Zealand Transport Agency

Chauhan B P, Joshi G and Parida P 2019 Car following model for urban signalised intersection to estimate speed based vehicle exhaust emissions *Urban Clim.* **29** 100480

Chevalier G, Le Ny J and Malhamé R 2015 A micro-macro traffic model based on mean-field games *2015 American Control Conf. (ACC)* (IEEE) pp 1983–8

Cohen M C, Jacquillat A, Ratzon A and Sasson R 2022 The impact of high-occupancy vehicle lanes on carpooling *Transp. Res. A* **165** 186–206

Colberg C A, Tona B, Stahel W A, Meier M and Staehelin J 2005 Comparison of a road traffic emission model (hbefa) with emissions derived from measurements in the gubrist road tunnel, switzerland *Atmos. Environ.* **39** 4703–14

Day C M, Ernst J M, Brennan T M, Chou C-S, Hainen A M, Remias S M, Nichols A, Griggs B D and Bullock D M 2012 Performance measures for adaptive signal control: case study of system-in-the-loop simulation *Transp. Res. Rec.* **2311** 1–15

De Coensel B, Can A, Degraeuwe B, De Vlieger I and Botteldooren D 2012 Effects of traffic signal coordination on noise and air pollutant emissions *Environ. Modelling Softw.* **35** 74–83

Department for Transport 2023 Road traffic statistics (available at: https://roadtraffic.dft.gov.uk/local-authorities/195) (Accessed 23 September 2023)

Din A U, Ming J, Rahman I U, Han H, Yoo S and Alhrahsheh R R 2023 Green road transportation management and environmental sustainability: the impact of population density *Heliyon* **9** e19771

Durrani U, Lee C and Maoh H 2016 Calibrating the wiedemann's vehicle-following model using mixed vehicle-pair interactions *Transp. Res. C* **67** 227–42

Fan J, Gao K, Xing Y and Lu J 2019 Evaluating the effects of one-way traffic management on different vehicle exhaust emissions using an integrated approach *J. Adv. Transp.* **2019** 6248796

Farrag S G, El-Hansali M Y, Yasar A U H, Shakshuki E M and Malik H 2020 A microsimulation-based analysis for driving behaviour modelling on a congested expressway *J. Ambient Intell. Human. Comput.* **11** 5857–74

Gallus J, Kirchner U, Vogt R and Benter T 2017 Impact of driving style and road grade on gaseous exhaust emissions of passenger vehicles measured by a portable emission measurement system (pems) *Transp. Res. D* **52** 215–26
Gazis D C, Herman R and Potts R B 1959 Car-following theory of steady-state traffic flow *Oper. Res.* **7** 499–505
Gipps P G 1981 A behavioural car-following model for computer simulation *Transp. Res. B* **15** 105–11
Göttlich S, Herty M and Ulke A 2024 Speed limits in traffic emission models using multi-objective optimization *Optim. Eng.* **26** 1–29
Grzybowska H, Wijayaratna K, Shafiei S, Amini N and Travis Waller S 2022 Ramp metering strategy implementation: a case study review *J. Transp. Eng. A* **148** 03122002
Harrison R M, Allan J, Carruthers D, Heal M R, Lewis A C, Marner B, Murrells T and Williams A 2021 Non-exhaust vehicle emissions of particulate matter and voc from road traffic: a review *Atmos. Environ.* **262** 118592
Hasnine M S, Aboudina A, Abdulhai B and Habib K N 2020 Mode shift impacts of optimal time-dependent congestion pricing in large networks: a simulation-based case study in the greater toronto area *Case Stud. Transp. Policy* **8** 542–52
Heydari S, Tainio M, Woodcock J and de Nazelle A 2020 Estimating traffic contribution to particulate matter concentration in urban areas using a multilevel bayesian meta-regression approach *Environ. Int.* **141** 105800
Irin S and Habib M A 2016 Microsimulation-based emissions modeling for a major infrastructure renewal plan: assessment of network attributes and land use effects on vehicular emissions *Transp. Res. Rec.* **2570** 127–38
Jalili S, Nallaperuma S, Keedwell E, Dawn A and Oakes-Ash L 2021 Application of metaheuristics for signal optimisation in transportation networks: a comprehensive survey *Swarm Evol. Comput.* **63** 100865
Jie L, Van Zuylen H, Chen Y, Viti F and Wilmink I 2013 Calibration of a microscopic simulation model for emission calculation *Transp. Res. C* **31** 172–84
Kessels F and Kessels F 2019 Mesoscopic models *Traffic Flow Modelling: Introduction to Traffic Flow Theory Through a Genealogy of Models* pp 99–106
Khondaker B and Kattan L 2015 Variable speed limit: an overview *Transp. Lett.* **7** 264–78
Klar A and Wegener R 2000 Vehicular traffic: From microscopic to macroscopic description *Transp. Theory Stat. Phys.* **29** 479–93
Kotsialos A, Papageorgiou M, Diakaki C, Pavlis Y and Middelham F 2002 Traffic flow modeling of large-scale motorway networks using the macroscopic modeling tool metanet *IEEE Trans. Intell. Transp. Syst.* **3** 282–92
Koupal J, Michaels H, Cumberworth M, Bailey C and Brzezinski D 2002 Epa's plan for moves: a comprehensive mobile source emissions model *Proc. 12th CRC On-Road Vehicle Emissions Workshop* (Citeseer) pp 15–17
Kousoulidou M, Fontaras G, Ntziachristos L, Bonnel P, Samaras Z and Dilara P 2013 Use of portable emissions measurement system (pems) for the development and validation of passenger car emission factors *Atmos. Environ.* **64** 329–38
Kővári B, Pelenczei B, Aradi S and Bécsi T 2022 Reward design for intelligent intersection control to reduce emission *IEEE Access* **10** 39691–9
Krauss S 1998 Microscopic modeling of traffic flow: Investigation of collision free vehicle dynamics *PhD Dissertation* Department of Mobility and System Technology, University of Cologne
Kumar P G, Lekhana P, Tejaswi M and Chandrakala S 2021 Effects of vehicular emissions on the urban environment-a state of the art *Mater. Today: Proc.* **45** 6314–20
Lee C, Hellinga B and Saccomanno F 2006 Evaluation of variable speed limits to improve traffic safety *Transp. Res. C* **14** 213–28
Li J-Q, Wu G and Zou N 2011 Investigation of the impacts of signal timing on vehicle emissions at an isolated intersection *Transp. Res. D* **16** 409–14
Li R, Dong L, Zhang J, Wang X, Wang W-X, Di Z and Stanley H E 2017 Simple spatial scaling rules behind complex cities *Nat. Commun.* **8** 1841
Lighthill M J and Whitham G B 1955 On kinematic waves II. A theory of traffic flow on long crowded roads *Proc. R. Soc. A* **229** 317–45
Lindau T (World Resources Institute) 2015 Transport plays a key role in urban air quality (available at: https://www.wri.org/insights/transport-plays-key-role-urban-air-quality#) (Accessed 26 September 2023)
Liu R, Van Vliet D and Watling D 2006 Microsimulation models incorporating both demand and supply dynamics *Transp. Res. A* **40** 125–50
Llopis-Castelló D, Pérez-Zuriaga A M, Camacho-Torregrosa F J and Garcia A 2018 Impact of horizontal geometric design of two-lane rural roads on vehicle co2 emissions *Transp. Res. D* **59** 46–57
Lopez P A, Behrisch M, Bieker-Walz L, Erdmann J, Flötteröd Y P, Hilbrich R, Lücken L, Rummel J, Wagner P and Wießner E 2018 Microscopic traffic simulation using sumo *The 21st IEEE Int. Conf. on Intelligent Transportation Systems* (IEEE)
Madireddy M, De Coensel B, Can A, Degraeuwe B, Beusen B, De Vlieger I and Botteldooren D 2011 Assessment of the impact of speed limit reduction and traffic signal coordination on vehicle emissions using an integrated approach *Transp. Res. D* **16** 504–8
Madziel M 2023 Vehicle emission models and traffic simulators: a review *Energies* **16** 3941
McDonald M, Wu J and Brackstone M 1997 Development of a fuzzy logic based microscopic motorway simulation model *Proc. Conf. on Intelligent Transportation Systems* (IEEE) pp 82–87
Meng D, Song G, Huang J, Lu H, Wu Y and Yu L 2024 Car-following model considering jerk-constrained acceleration stochastic process for emission estimation *Physica A* **639** 129670
Meng D, Song G, Wu Y, Zhai Z, Yu L and Zhang J 2021 Modification of Newell's car-following model incorporating multidimensional stochastic parameters for emission estimation *Transp. Res. D* **91** 102692
Midenet S, Boillot F and Pierrelée J-C 2004 Signalized intersection with real-time adaptive control: on-field assessment of CO_2 and pollutant emission reduction *Transp. Res. D* **9** 29–47
Mohebifard R and Hajbabaie A 2019 Optimal network-level traffic signal control: a benders decomposition-based solution algorithm *Transp. Res. B* **121** 252–74
Ngoduy D and Maher M 2012 Calibration of second order traffic models using continuous cross entropy method *Transp. Res. C* **24** 102–21
Notter B, Hausberger S, Matzer C U, Weller K, Dippold M, Politschnig N and Lipp S 2021 HBEFA 4.2 - documentation of updates *Technical Report*, INFRAS
Panwai S and Dia H 2007 Neural agent car-following models *IEEE Trans. Intell. Transp. Syst.* **8** 60–70
Payne H 1971 *Models of Freeway Traffic and Control. Mathematical Models of Public Systems. Simulation Councils* (Inc., Vista)
Pipes L A 1953 An operational analysis of traffic dynamics *J. Appl. Phys.* **24** 274–81
Pourabdollah M, Bjärkvik E, Fürer F, Lindenberg B and Burgdorf K 2017 Calibration and evaluation of car following models using real-world driving data *2017 IEEE 20th Int. Conference on Intelligent Transportation Systems (ITSC)* (IEEE) pp 1–6
Rabl A and De Nazelle A 2012 Benefits of shift from car to active transport *Transp. Policy* **19** 121–31
Reuschel A 1950 Fahrzeugbewegungen in der kolonne *Osterreichisches Ingenieur Archiv* **4** 193–215

Richards P I 1956 Shock waves on the highway *Oper. Res.* **4** 42–51
Rodríguez R A, Virguez E A, Rodríguez P A and Behrentz E 2016 Influence of driving patterns on vehicle emissions: a case study for latin american cities *Transp. Res. D* **43** 192–206
Scora G and Barth M 2006 Comprehensive modal emissions model (CMEM), version 3.01 *User Guide* Centre for environmental research and technology. University of California, Riverside
Shahgholian M and Gharavian D 2018 Advanced traffic management systems: an overview and a development strategy (arXiv:1810.02530)
Shaikh P W, El-Abd M, Khanafer M and Gao K 2020 A review on swarm intelligence and evolutionary algorithms for solving the traffic signal control problem *IEEE Trans. Intell. Transp. Syst.* **23** 48–63
Shang R, Zhang Y and Shen Z J M 2021 Analyzing the effects of road type and rainy weather on fuel consumption and emissions: a mesoscopic model based on big traffic data *IEEE Access* **9** 62298–315
Song G, Yu L and Geng Z 2015 Optimization of Wiedemann and Fritzsche car-following models for emission estimation *Transp. Res. D* **34** 318–29
Song G, Yu L and Xu L 2013 Comparative analysis of car-following models for emissions estimation *Transp. Res. Rec.* **2341** 12–22
Stevanovic A, Stevanovic J, Zhang K and Batterman S 2009 Optimizing traffic control to reduce fuel consumption and vehicular emissions: integrated approach with VISSIM, CMEM and VISGAOST *Transp. Res. Rec.* **2128** 105–13
Tampère C M 2004 Human-kinetic multiclass traffic flow theory and modelling. With application to advanced driver assistance systems in congestion *PhD Thesis* Delft University of Technology
Toledo T 2007 Driving behaviour: models and challenges *Transp. Rev.* **27** 65–84
Treiber M, Hennecke A and Helbing D 2000 Congested traffic states in empirical observations and microscopic simulations *Phys. Rev. E* **62** 1805
Treiber M, Kesting A and Helbing D 2006 Delays, inaccuracies and anticipation in microscopic traffic models *Physica A* **360** 71–88
United Nations 2019 United nations announces 2019 climate action summit 'clean air initiative', calls on governments at all levels to join *Technical Report* United Nations
United Nations 2024 Cities and climate change (available at: www.unep.org/explore-topics/resource-efficiency/what-we-do/cities-and-climate-change)
Wiedemann R 1974 Simulation des strassenverkehrsflusses *Technical Report* University Karlsruhe
Wyatt D W, Li H and Tate J E 2014 The impact of road grade on carbon dioxide (co2) emission of a passenger vehicle in real-world driving *Transp. Res. D* **32** 160–70
Xu Y, Jiang S, Li R, Zhang J, Zhao J, Abbar S and González M C 2019 Unraveling environmental justice in ambient $PM_{2.5}$ exposure in Beijing: a big data approach *Comput. Environ. Urban Syst.* **75** 12–21
Yan X, Wu Z and Wang H 2023 Network noise control under speed limit strategies using an improved bilevel programming model *Transp. Res. D* **121** 103805
Zhang C, Chung E, Sabar N R, Bhaskar A and Ma Y 2023 Optimisation of variable speed limits at the freeway lane drop bottleneck *Transp. A* **19** 2033878
Zhang G, Chang F, Jin J, Yang F and Huang H 2024 Multi-objective deep reinforcement learning approach for adaptive traffic signal control system with concurrent optimization of safety, efficiency and decarbonization at intersections *Acc. Anal. Prevent.* **199** 107451
Zhang H M 2002 A non-equilibrium traffic model devoid of gas-like behavior *Transp. Res. B* **36** 275–90
Zhao B, Lin Y, Hao H and Yao Z 2022 Fuel consumption and traffic emissions evaluation of mixed traffic flow with connected automated vehicles at multiple traffic scenarios *J. Adv. Transp.* **2022** 6345404
Zhao H, He R and Jia X 2019 Estimation and analysis of vehicle exhaust emissions at signalized intersections using a car-following model *Sustainability* **11** 3992
Zong F, Zeng M and Li Y-X 2024 Congestion pricing for sustainable urban transportation systems considering carbon emissions and travel habits *Sustain. Cities Soc.* **101** 105198